Neuron, Vol. 47, 57–69, July 7, 2005, Copyright ©2005 by Elsevier Inc. DOI 10.1016/j.neuron.2005.05.030

Opposing Gradients of Ephrin-As and EphA7 in the Superior Colliculus Are Essential for Topographic Mapping in the Mammalian Visual System

Tahira Rashid,[1] A. Louise Upton,[2] Aida Blentic,[1] Thomas Ciossek,[3,4] Bernd Knöll,[1,5] Ian D. Thompson,[2] and Uwe Drescher[1,*]

[1]MRC Centre for Developmental Neurobiology
King's College London
New Hunt's House
Guy's Hospital Campus
London SE1 1UL
United Kingdom

[2]University Laboratory of Physiology
Parks Road
Oxford OX1 3PT
United Kingdom

[3]Max-Planck-Institute for Developmental Biology
Spemannstraße 35
72076 Tübingen
Germany

Summary

During development of the retinocollicular projection in mouse, retinal axons initially overshoot their future termination zones (TZs) in the superior colliculus (SC). The formation of TZs is initiated by interstitial branching at topographically appropriate positions. Ephrin-As are expressed in a decreasing posterior-to-anterior gradient in the SC, and they suppress branching posterior to future TZs. Here we investigate the role of an EphA7 gradient in the SC, which has the reverse orientation to the ephrin-A gradient. We find that in EphA7 mutant mice the retinocollicular map is disrupted, with nasal and temporal axons forming additional or extended TZs, respectively. In vitro, retinal axons are repelled from growing on EphA7-containing stripes. Our data support the idea that EphA7 is involved in suppressing branching anterior to future TZs. These findings suggest that opposing ephrin-A and EphA gradients are required for the proper development of the retinocollicular projection.

Introduction

The retinocollicular/tectal projection represents a long-standing model system in which to study the mechanisms and molecules involved in controlling axon guidance in the target area. Retinocollicular/tectal mapping is topographically organized such that neighboring cells in the projecting area are connected to neighboring cells in the target area. In the retinocollicular projection of rodents, nasal and temporal axons project to the posterior and anterior superior colliculus (SC), respectively, while, in the perpendicular axis, dorsal and ventral retinae are connected to the lateral and medial SC.

Retinocollicular mapping is a multistep process of interwoven activity-independent and -dependent processes. It is believed that, initially, a coarse, activity-independent map forms, driven by gradients of axon guidance ligands in the SC and corresponding receptors in the retina, which provide directional and positional information for ingrowing axons (Sperry, 1963). While the involvement of guidance gradients is undisputable, there is an ongoing discussion about their precise role in forming topographic maps (for an overview, see Loschinger et al., 2000). On the one side, two or more gradients with opposing effects on retinal axons have been proposed, with axons forming termination zones (TZs) in that region of the SC where the combined effects of these gradients lead to either a minimum or maximum of a "guidance parameter" (Gierer, 1983; Yates et al., 2001). On the other side, it has been argued that ingrowing axons themselves impose a topographic map onto the target area, requiring target gradients only to orient this map (Willshaw and von der Malsburg, 1976).

Topographic mapping is a dynamic process in which the relative expression levels of guidance receptor(s) and the competition between axons play major roles (Brown et al., 2000; Feldheim et al., 2004; Feldheim et al., 2000; Goodhill, 2000; Goodhill and Richards, 1999; Reber et al., 2004). Activity-dependent processes are necessary to form the mature, precise map (for reviews, see Debski and Cline, 2002; Katz and Shatz, 1996), and inhibition of correlated activity-dependent processes in the retina results in a less-sharp topographic projection and less-dense TZs (McLaughlin et al., 2003a).

In mouse and chick embryos, in contrast to other species, such as fish and frog, retinal axons grow into the superior colliculus initially in a nontopographic manner both anteroposteriorly and mediolaterally, significantly overshooting their future TZs and eventually approaching the posterior end of the SC at around the time of birth (Figure 1A; Nakamura and O'Leary, 1989; Simon and O'Leary, 1992). The development of a crude topographic map is initiated through interstitial branching and arborization (Simon and O'Leary, 1992; Yates et al., 2001), which are thought to be dependent on an interplay between branch-promoting and branch-suppressing activities (see, for example, Cohen-Cory, 1999; Cohen-Cory and Fraser, 1995; O. Choi and D.D. O'Leary, 1999, Soc. Neurosci., abstract). Thus, after growing into the SC between about E16 and P1, retinal axons send out branches from the beginning preferentially at their future TZs, with little branching occurring anterior or posterior to it. Further branching and arborization contribute to the formation of mature TZs over the following days, while aberrant axon segments and branches are eliminated. This process is completed at around P8 (Figure 1A; Simon and O'Leary, 1992).

Members of the Eph family of receptor tyrosine ki-

*Correspondence: uwe.drescher@kcl.ac.uk

[4]Present address: ALTANA Pharma AG, Byk-Gulden-Str. 2, 78467 Konstanz, Germany.

[5]Present address: Institute for Cell Biology, Department of Molecular Biology, University of Tübingen, Auf der Morgenstelle 15, 72076 Tübingen, Germany.

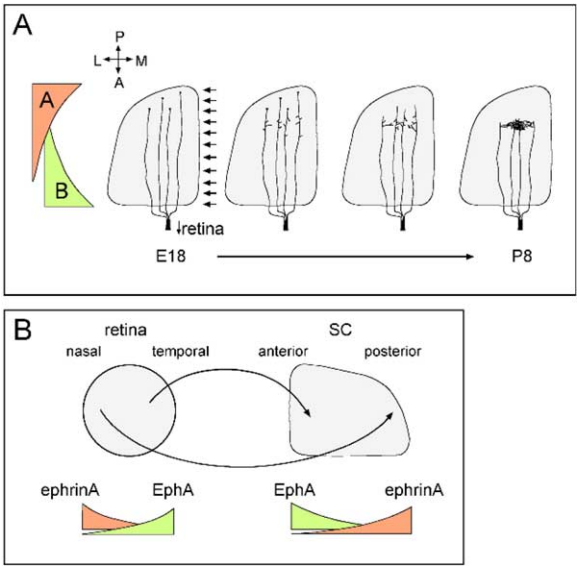

Figure 1. Development of the Retinocollicular Projection in Mouse

(A) Retinal axons grow in a nontopographic manner into the SC: individual axons substantially overshoot their future TZs and eventually approach the posterior pole of the SC at about E18. Subsequently, TZs develop through interstitial branching and arborizations (McLaughlin et al. [2003b]). The model shown here proposes that the position of a TZ is determined through an interplay between a uniformly distributed branch-promoting activity (arrows) and topographically expressed activities controlling branching anterior and posterior to the future TZ (shown in red and green on the left side).

(B) In the retinocollicular projection, temporal and nasal axons project onto the anterior and posterior SC, respectively. Expression patterns of EphAs and ephrin-As in the retina and SC during development of this projection are schematized. The expression patterns of members of the EphB family are not shown; for details, see McLaughlin et al. (2003b).

nases and their ephrin ligands play important roles in the development of the retinotectal/collicular projection (for review, see Wilkinson, 2000; McLaughlin et al., 2003b). Crucial to an understanding of the functions of the Eph family is their capacity for bidirectional signaling, such that Ephs and ephrins can function both as receptors and ligands (Kullander and Klein, 2002; Knöll and Drescher, 2002).

In mouse, EphA5 and EphA6 are expressed more strongly on temporal than on nasal axons, while ephrin-A2 and ephrin-A5 are expressed at higher levels in the posterior than in the anterior part of the SC (Feldheim et al., 2000; Frisen et al., 1998; Reber et al., 2004). Due to the repellent EphA^{retina}/ephrin-A^{SC} interactions, temporal axons project onto the anterior SC as formation of TZs in the posterior SC is suppressed by the posterior > anterior expression of ephrin-As. Thus, the higher the expression of EphAs is on retinal axons, the more the formation of TZs is "pushed" toward the anterior SC. In *ephrin-A5*$^{-/-}$ and *ephrin-A2*$^{-/-}$*/ephrin-A5*$^{-/-}$ mice—and similarly in *EphA5*$^{lacZ/lacZ}$ mice (in which the kinase domain of EphA5 is replaced by lacZ)—additional TZs are formed by temporal axons in more posterior regions of the SC (Feldheim et al., 2004, 2000; Frisen et al., 1998). This appears to be caused in *ephrin-A2*$^{-/-}$*/ephrin-A5*$^{-/-}$ mice by a posterior SC that is less inhibitory for branching, and in *EphA5*$^{lacZ/lacZ}$ mice by temporal axons that are less sensitive to the branch-suppressing activity of ephrin-As (Feldheim et al., 2004, 2000). In the stripe assay, temporal axons form more branches on anterior than on posterior tectal membranes, an activity which can be abolished by adding soluble EphA-Fc—an indication of the involvement of the EphA system in this process (Roskies and O'Leary, 1994; Yates et al., 2001). Thus, gradients of EphAs in the retina and ephrin-As in the SC (EphA^{retina}, ephrin-A^{SC}) might suppress branching posterior to future TZs.

At the same time, these activities cannot account for a control of branching anterior to the future TZ, leading to the question of which factors might be involved in this activity. Besides other possibilities, such a factor could be a branch-suppressing activity expressed in a countergradient to the ephrin-A^{SC} gradient, or it could be a branch-promoting activity expressed in a gradient parallel to the ephrin-A^{SC} gradient. With regard to the latter possibility, it is also conceivable that the ephrin-A^{SC} gradient is being read by some other retinal EphAs, which mediate a branch-promoting activity (see also Yates et al., 2001; Hansen et al., 2004).

Interestingly, EphAs are also expressed in gradients in the superior colliculus (anterior > posterior), and ephrin-As are expressed in the retina (nasal > temporal) (Figure 1B). Given the capacity for bidirectional signaling within the EphA family, it is plausible that ephrin-As might function as receptors on retinal axons ("reverse signaling") and EphAs as the corresponding ligands in the SC. The orientation of these gradients makes ephrin-As^{retina}/EphAs^{SC} good candidates for the postulated branch-suppressing activity anterior to TZs.

Here we set out to analyze the topographic projection in mice mutant for EphA7, which shows the strongest and most pronounced differential expression (anterior > posterior) in the SC and which is not expressed in the retina. Our data show that, in *EphA7*$^{-/-}$ mice, topographic mapping of both temporal and nasal axons is disturbed and that EphA7 is a repellent substrate for retinal axon growth in vitro. This supports a model in which the ephrin-A^{retina}/EphA^{SC} pair is part of the countergradient system to the EphA^{retina}/ephrin-A^{SC} system involved in controlling retinocollicular mapping.

Results

Expression Pattern of EphAs in the Superior Colliculus

To investigate the function of EphAs in the SC, we first analyzed their expression patterns during a critical phase of development of the retinocollicular projection by RNA in situ hybridization experiments. At P1, EphA3 and EphA7 exhibit anterior > posterior gradients in the SC (Figures 2C and 2E). Compared to EphA7, EphA3 expression appears to be weaker and confined more to the anterior SC. EphA4 is broadly expressed at high levels and shows only a very shallow, if any, gradient (Figure 2D), while EphA2, EphA5, and EphA6 are not, or are only very weakly, expressed (data not shown). EphA8 expression was reported only in a small con-

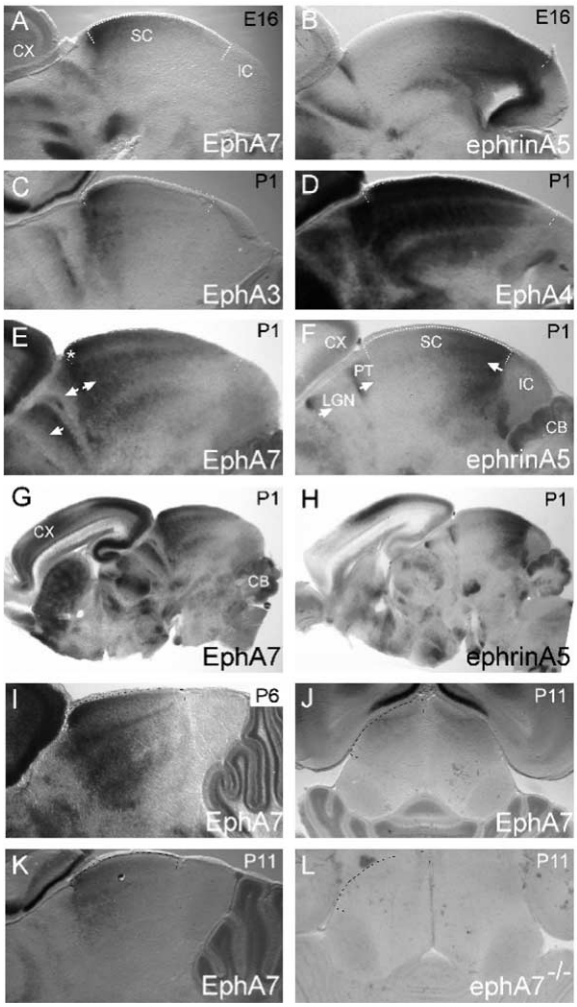

Figure 2. RNA In Situ Hybridization Analysis of EphA Family Members during Development of the Retinocollicular Projection

Expression at E16 of EphA7 (A) and ephrin-A5 (B) in sagittal sections of the midbrain. Expression of EphA3 (C), EphA4 (D), EphA7 (E), and ephrin-A5 (F) at P1 in sagittal sections of the SC. In (F), the location of the SC, the inferior colliculus (IC), the pretectum (PT), and the lateral geniculate gyrus (LGN) are indicated. In (E), the superficial layers of the SC, which receive retinal input, are marked with * (compare with Figures 3E and 3F). The various gradients of EphA7 and ephrin-A5 are indicated in (E) and (F) by arrows. Expression of EphA7 (G) and ephrin-A5 (H) at P1 in sagittal sections of the entire brain. Expression of EphA7 at P6 (I) and P11 (J and K) in horizontal (J) and sagittal (K) sections. These data indicate that EphA7 is expressed in the SC in an anterior > posterior gradient throughout the development of the retinocollicular projection, and is strongly downregulated after its maturation. (L) P11 horizontal sections from *EphA7*$^{-/-}$ mice analyzed for EphA7-specific transcripts. In (A)–(F) and (I)–(L), the SC is indicated by dashed lines. PT, pretectum; LGN, lateral geniculate gyrus; SC, superior colliculus; IC, inferior colliculus; CB, cerebellum; CX, cortex.

fined area approximately in the center of the SC (Park et al., 1997), while EphA1 is not expressed in the brain at all (Zhou, 1998). Thus, it appears that with regard to EphA expression in the SC, EphA7 displays a particularly interesting pattern. We have therefore analyzed its expression pattern throughout the development of the retinocollicular system and have compared it with ephrin-A5, which is known to be expressed in a posterior > anterior gradient in the SC (Figures 2B, 2F, and 2H) (Frisen et al., 1998).

At E16, when retinal axons have started to invade the SC, EphA7 is expressed in an anterior > posterior gradient stretching through the entire midbrain/SC (Figure 2A; Ciossek et al., 1995). This expression pattern remains unchanged up to at least P6 (Figure 2I), with EphA7 becoming barely detectable at P11 (Figures 2J and 2K). Thus, EphA7 is expressed at critical times during formation of the retinocollicular projection and is subsequently downregulated. EphA7 is expressed in the superficial layers of the SC (Figures 2E and 2I), i.e., the stratum griseum superficiale (SGS), and is therefore in layers that are in contact with ingrowing retinal axons and receive retinal input (see also Figures 3E and 3F). These RNA data correlate well with EphA7 Western blot analyses of SC and retinae from P1 mice (Figure 4D), showing a clear differential expression of EphA7 protein between the anterior and posterior SC, and no expression in the retina (Figure 4D; see also Ciossek et al., 1995). Thus, EphA7 is expressed at the right time and in the right place to play a role in guiding retinal axons to their correct topographic position.

Interestingly, the countergradients of ephrin-As and EphAs are not only seen in the SC, but also in other target areas of retinal axons, such as the pretectum and the lateral geniculate nucleus (LGN) (Figures 2E–2H, arrows in Figures 2E and 2F; Feldheim et al., 1998; Marin et al., 2001). The idea has been put forward that topographic guidance to different target fields might be under the control of the same set of ephrin-A guidance molecules (Feldheim et al., 1998; Marin et al., 2001). Thus, in an extension, ephrin-A *and* EphA countergradients might play such a role in retinal target areas. Another striking set of countergradients is seen in the cortical plate, where a bidirectional gradient of ephrin-A5 in the somatosensory cortex is juxtaposed to EphA7 gradients both anterior and posterior to it (Figures 2G and 2H; Mackarehtschian et al., 1999; Yun et al., 2003).

Next we investigated the retinal expression of ephrin-As by staining explants from E16.5 mouse retina with EphA7-Fc (Figures 3A–3D). Here nasal axons showed a stronger ephrin-A expression than temporal axons (Figures 3A and 3B; Hornberger et al., 1999). This differential expression correlates well with data from staining flat mounts of mouse retina (Marcus et al., 1996) and from the functional characterization of retinal ephrin-A expression in *ephrin-A2*$^{-/-}$, *ephrin-A5*$^{-/-}$ mice (Feldheim et al., 2000). Retinal axons from chick and zebrafish show a similar differential expression of ephrin-As (data not shown; Brennan et al., 1997; Connor et al., 1998; Hornberger et al., 1999), underscoring the evolutionary conservation of differential expression of ephrin-As in the retina (Figure 1).

Generation and Characterisation of *EphA7*$^{-/-}$ Mice

Based on these intriguing expression patterns, EphA7 appears to be a prime candidate to aid the investigation of the role of collicular expression of EphAs in retinocollicular mapping. We have generated mice carrying a null mutation in the gene encoding EphA7 by homolo-

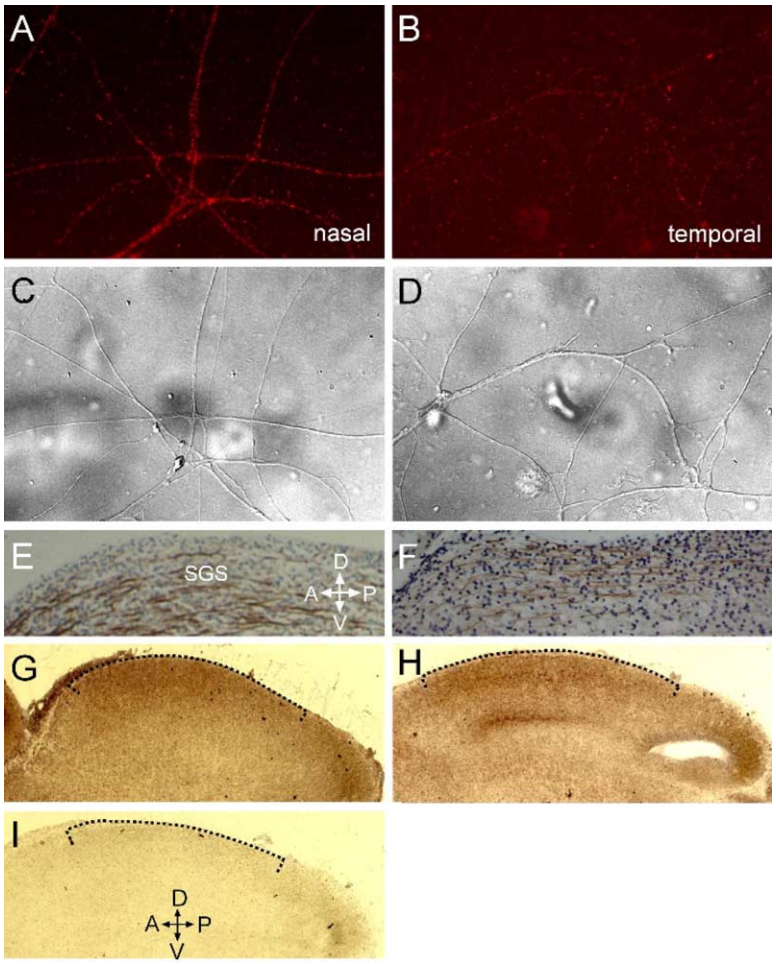

Figure 3. Protein Expression Patterns of EphA Family Members

(A–D) Staining of E16.5 nasal (A) and temporal (B) axons from mouse retinal explants for ephrin-A expression using EphA7-Fc. Corresponding bright-field pictures are shown in (C) and (D). Ephrin-As are more strongly expressed on nasal than on temporal axons.

(E and F) Analysis of retinal axon tracts in wild-type (E) and *EphA7*$^{-/-}$ (F) mice by staining P1 sagittal sections with an anti-neurofilament antibody (brown). Retinal axons grow from the ventrally located chiasm along the thalamus toward the SC and invade it from the anterior pole, then growing toward its posterior pole. Ingrowth of retinal axons into the SC within the superficial layers is indistinguishable between wild-type and *EphA7*$^{-/-}$ mice. Cell nuclei are visualized by staining with haematoxylin (blue) to highlight the overall structure and layering of the SC. Anterior is to the left and dorsal to the top. SGS, stratum griseum superficiale.

(G–I) Expression of EphA proteins analyzed on parasagittal sections of the SC from E15.5 mice as revealed by a staining protocol using ephrin-A5-Fc and AP-coupled anti-Fc antibodies (Conover et al., 2000). (G) Wild-type mice, (H) *EphA7*$^{-/-}$ mice, (I) staining using Fc alone. Using ephrin-A5-Fc, "free" EphAs available for interaction with retinal ephrin-As can be identified. The extent of the SC is indicated by a dotted line. Anterior is to the left and dorsal to the top.

gous recombination in which the first exon containing the start codon and signal peptide has been removed (Figure 4A). Homologous recombination was verified by Southern blot analysis (Figure 4B). *EphA7*$^{-/-}$ mice were also characterized by RT-PCR analysis of RNA from brain of adult mice (Figure 4C), by RNA in situ hybridization (Figure 2L), by Western blot analysis of immunoprecipitates from retina, and SC using an EphA7-specific antibody (Figure 4D). These data show the lack of EphA7-specific RNA and protein in these mice, indicating that the homologous recombination has led to the complete abolishment of EphA7 expression. *EphA7*$^{-/-}$ mice reach adulthood, are fertile, and show no gross morphological or behavioral defects.

We addressed the question of whether abolishment of EphA7 expression would have any gross effects on the development of the SC. For this, we have compared the mRNA expression pattern of EphAs and ephrin-As in *EphA7*$^{-/-}$ mice to that of wild-type mice (see Figure S1 in the Supplemental Data online). These data show that abolishment of EphA7 expression does not change the expression pattern of other EphA family members, from which we infer that the general patterning of the SC is not disturbed in *EphA7*$^{-/-}$ mutant mice. We have also compared retinal axon tracts from wild-type and *EphA7*$^{-/-}$ mutant mice by neurofilament immunostaining of corresponding sections (Figures 3E and 3F). Here, no abnormalities regarding, for example, pathfinding errors, fasciculation defects, or premature termination of axon growth were found.

We then investigated the EphA protein gradient by using ephrin-A5-Fc as a probe. Our data show an anterior > posterior gradient of EphAs in the SC of both wild-type and *EphA7*$^{-/-}$ mice (Figures 3G–3I). Use of ephrin-A5-Fc uncovers the gradient of "free" EphAs, which are accessible to interaction with ephrin-As on retinal axons. Staining with ephrin-A-Fcs followed by AP-coupled anti-Fc antibodies, however, did not allow a thorough quantification of differences in EphA protein amounts between wild-type and mutant mice. Nevertheless, it appears that the overall intensity of staining was less strong in mutant than wild-type mice.

Analysis of Topographic Patterning in *EphA7*$^{-/-}$ Mice by Anterograde Tracing

To investigate possible topographic mapping defects, small focal injections of DiI were made at either the ventronasal or dorsotemporal pole in the retina of wild-type or *EphA7*$^{-/-}$ mice, followed 24–48 hr later by examination of the contralateral SC (Figure 5). This time interval is sufficient to allow transfer of DiI from the labeled cell bodies and axons in the retina along the fiber

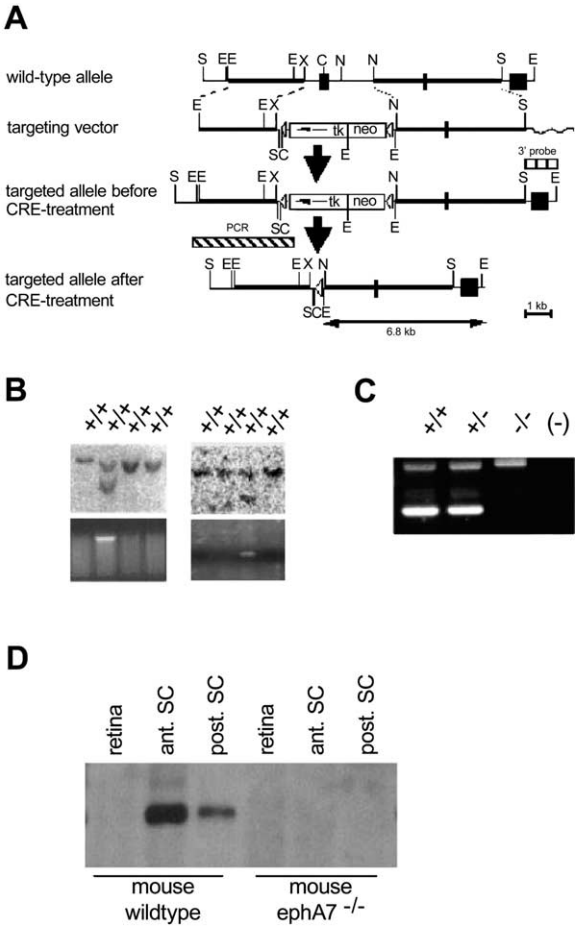

Figure 4. Targeted Disruption of the EphA7 Gene

(A) Partial map of the *EphA7* genomic locus with the targeting construct and the resulting targeted loci. The EphA7 targeting vector was designed to replace exon I (1–330 bp of the EphA7 cDNA), including part of the upstream sequence (–601 to –1), with a loxP-flanked tk/neo selection cassette. For homologous recombination, the 5′ EcoRI-XhoI 3 kb sequence and 3′ NotI-SalI 5.3 kb sequence flanking this region were subcloned into pBluescript vector. Homologous recombination would delete the upstream sequence and exon I coding for the signal sequence of EphA7, resulting in a null allele. In order to remove the tk/neo selection cassette, positive ES cells were transfected with an expression construct for Cre recombinase. The probe used for all Southern blot analyses was a 1.3 kb genomic fragment containing exon III (395–1063 bp). The marked area (PCR′) denotes the amplified sequence used to verify the 5′ region of the targeted allele (3.6 kb). C, ClaI; E, EcoRI; N, NotI; S, SalI; X, XhoI; neo, neomycin gene; tk, thymidine kinase gene.

(B) Genotype analysis of EphA7 homozygous (+/+) and heterozygous (+/–) ES cells before (upper left panel) and after (upper right panel) the transfection with the Cre recombinase expression plasmid. Genomic DNA was isolated, digested with EcoRI, and subjected to Southern blot analysis using the 3′ external probe shown in (A). Alleles bearing the *EphA7* mutation show a 6.8 kb band, whereas a 9.7 kb band is observed in the wild-type alleles. For PCR analysis, primer pairs amplifying a 3.6 kb (lower left panel, see also [A]) or a 0.5 kb (lower right panel) band in the case of successful recombination were used.

(C) RT-PCR analysis of total RNA isolated from brains of adult animals of the indicated genotypes. Primers were chosen to amplify part of exon I of EphA7 (314 bp). –, no template control.

(D) Expression of EphA7 protein in wild-type and *EphA7*$^{-/-}$ mice. Same amounts of lysates from retina and anterior and posterior halves of the SC from wild-type and *EphA7*$^{-/-}$ mice were immunoprecipitated with an EphA7-specific monoclonal antibody using standard protein-biochemistry protocols. Immunoprecipitates were probed in a Western blot analysis for the presence of EphA7. In agreement with RNA in situ expression data (Figure 2), in wild-type mice, EphA7 protein is more strongly expressed in the anterior than the posterior SC. No expression was detected in the retina of either wild-type or *EphA7*$^{-/-}$ mice. The same data as shown here were obtained in three independently performed experiments.

Additional characterizations of *EphA7*$^{-/-}$ mice are shown in Figure 2L (in situ RNA analysis at P11), Figure 3F (axon staining in the SGS of SC), and Figures 3G–3I (expression of EphA proteins).

tracts to the area of the SC where the TZs of these cells/axons have developed. A comparison of the location of DiI in the retina and the TZ in the SC allows a judgement to be made about the formation of proper topographic projections. These analyses were done on P10–P14 mice, which is some number of days after maturation of the retinocollicular projection at about P8 (Hindges et al., 2002; Simon and O'Leary, 1992), in order to exclude the possibility that mapping defects are due to a delayed maturation of the topographic map in *EphA7*$^{-/-}$ mice.

In wild-type mice, nasal axons developed TZs only in the medioposterior SC (Figure 5H; Table 1). In contrast, we observed topographic targeting errors in *EphA7*$^{-/-}$ mice (Figures 5 and 8; Table 1): in about 62% of these mice, axons from the ventronasal retina formed—in addition to a TZ at the expected topographic location in the medioposterior SC—ectopic TZs (eTZs) in the medioanterior part of the SC (Figures 5B, 5C, 5E, and 5F; Figure 8; Table 1). Ectopic TZs in *EphA7*$^{-/-}$ mice were found consistently in the medioanterior SC and were less well developed than the TZs at the correct topographic position. The eTZs were found in the more anterior SC, but clearly within the SC and not directly at its border. Closer inspection allowed us to trace axons entering these eTZs and revealed a dense network of arborizations (Figures 5C and 5F).

In these DiI tracing experiments, temporal axons in *EphA7*$^{-/-}$ mice did not show obvious alterations; thus, axons from the dorsotemporal retina in wild-type and *EphA7*$^{-/-}$ mice map to the lateral-anterior SC (data not shown; Table 1).

Analysis of Retinocollicular Mapping in *EphA7*$^{-/-}$ Mice by Retrograde Tracing

The topographic targeting errors of nasal retinal axons in *EphA7*$^{-/-}$ mice were furthermore analyzed by retrograde tracing techniques (Figure 6). A single injection of fluorescent latex microspheres was made into the superficial layers of the anterior quarter of the SC of P14–P18 wild-type and *EphA7*$^{-/-}$ mutant mice. The microspheres are retrogradely transported by RGC axons to their cell bodies in the retina. Twenty-four to 48 hr later, the positions of labeled RGCs in the retinae of these animals were determined, while that of the injection site in the anterior SC was verified by sectioning of the SC (Figure 6; for details, see Experimental Procedures). In wild-type mice we found the expected topographic correlation: labeling of a small part of the anterior SC resulted in a patch of labeled RGCs only in the temporal retina (n = 7) (Figures 6A and 6B). Bigger

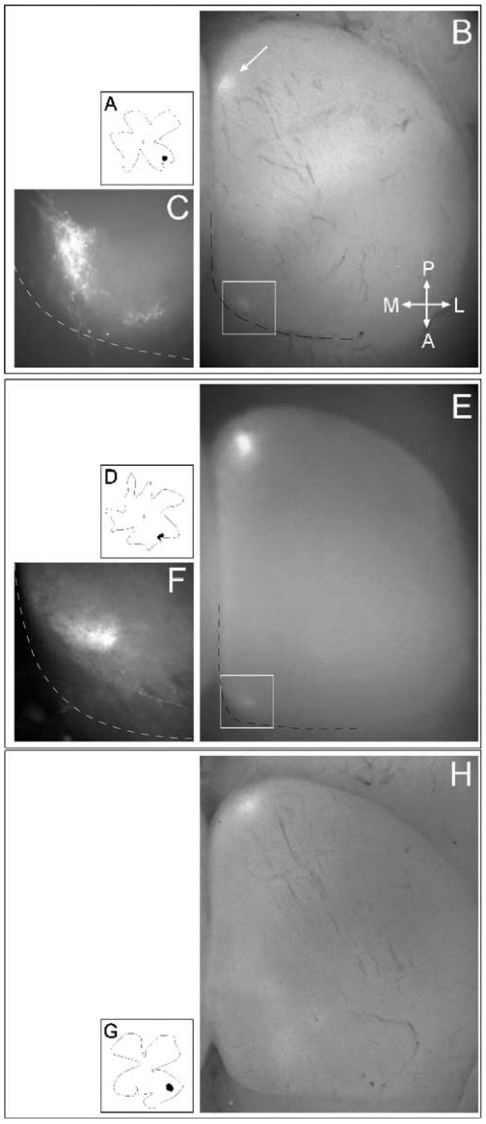

Figure 5. Topographic Targeting Errors of Nasal Retinal Axons in *EphA7*$^{-/-}$ Mice

One day after a focal injection of DiI into the ventronasal part of the retina of wild-type and *EphA7*$^{-/-}$ mice, retina and SC were prepared, and the location of DiI in the retina and of the TZs in the SC were determined. (A) Schematic drawing of a flat-mounted retina from an EphA7 mutant mouse. The location of DiI is indicated by a dot. Nasal is to the right, dorsal to the top. (B) The SC contralateral to this retina is shown in a dorsal view. A TZ in the medioposterior part of the SC (arrow) is formed at the topographically appropriate position. In addition, an eTZ in the medioanterior SC has formed. (C) Enlargement of this eTZ. (D–F) Analysis of another *EphA7*$^{-/-}$ mouse. Again, the locations of DiI in the retina (D) and of the normal TZ (E) and the eTZ (E and F) are shown. (G and H) In wild-type mice, DiI labeling of ventronasal axons (G) results in the formation of only one TZ in the topographically correct location in the medioposterior part of the SC (H). The anterior border of the SC is outlined by a dotted line. A summary of all DiI experiments is shown in Table 1. For retinae shown in (A), (D), and (G), nasal is to the right and dorsal to the top; for the SC shown in (B), (C), (E), (F), and (H), posterior is to the top and medial to the left. A, anterior; P, posterior; M, medial; L, lateral.

Table 1. Disturbance of Retinocollicular Mapping in *EphA7*$^{-/-}$ Mice as Analyzed by Anterograde Tracing

	EphA7$^{-/-}$	Wild-Type
Ventronasal axons		
total number of mice analyzed	13	21
with eTZ	8 (62%)	—
without eTZ	5	21
Dorsotemporal axons		
total number of mice analyzed	6	8
with eTZ	—	—
without eTZ	6	8

injections did tend to result in a higher number of scattered cells in nasal retina (e.g., Figure 6B). In contrast, in *EphA7*$^{-/-}$ mice we observed a disturbance of the retinocollicular map (Figures 6C and 6D), in agreement with the data obtained by anterograde tracing (see above). Thus, in some of the EphA7 mutant mice (3 out of 5), we found, in addition to a prominent label at the topographically correct position in the temporal retina, a *distinct* patch of labeled RGCs in the topographically inappropriate nasal retina (Figures 6C and 6D). In both cases, the nasal focus is clearly separate from the temporal focus, even in Figure 6D, in which a larger injection site is associated with increased scatter of labeled cells in temporal retina.

We quantified the distribution of labeled RGCs by generating isodensity contours of the labeled RGCs and measuring the area of the retina within the 5% or 20% contour line, which delineates those parts of the retina having a density of labeled cells greater than 5% or 20% of the maximum density of labeled cells. (Densities reflect cell numbers per sample square at different sample grid locations, and the contour plots were generated by using distance-weighted least-squares smoothing, see Experimental Procedures. The areas were not normalized for injection site size, see below.) This method revealed ectopic foci in the 5% contour lines in 3 out of 5 retinae from *EphA7*$^{-/-}$ mice, while no such 5% peak density lines other than the main focus were identified in wild-type mice (Figure 6).

Intriguingly, a quantification of the label in temporal retina (Figure 6) by measurement of the size of the area enclosed by the 5% and 20% peak density lines showed a statistically significant increase in the size of the foci of temporal axons from *EphA7*$^{-/-}$ mice compared to that of wild-type mice. For the 5% peak density contour, the means were 6.2% ± 1.0% of the total retinal area of wild-type retinae (n = 7) and 14.0% ± 2.5% for *EphA7*$^{-/-}$ retinae (n = 5; two-tailed $p < 0.01$). For the 20% contour, the respective means were 1.9% ± 0.4% for wt (n = 7) and 6.6% ±1.9% for *EphA7*$^{-/-}$ (n = 5; $p < 0.03$). These differences between wild-type and *EphA7*$^{-/-}$ mice in the extent of retinal labeling could not be explained by differences in the size of the SC injection site (2.4% ± 1.0% of the SC area for wild-type mice versus 2.8% ± 1.0% for *EphA7*$^{-/-}$ mice). This indicates that not only the projection pattern of nasal retinal axons but also that of temporal axons is affected in *EphA7*$^{-/-}$ mice. The increased foci seen in retrograde

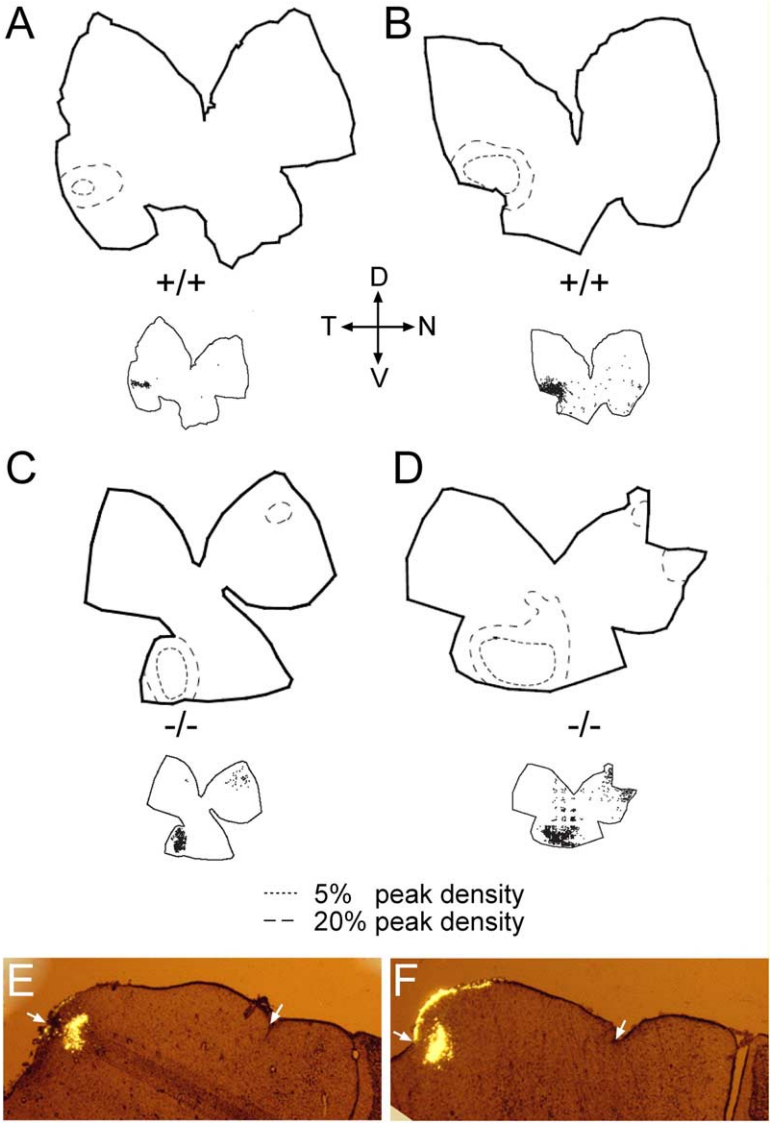

Figure 6. Topographic Targeting Errors in EphA7$^{-/-}$ Mice Analyzed by Retrograde Tracing

Fluorescent latex beads were injected into the anterior quarter of the SC of P14–P18 wild-type and *EphA7*$^{-/-}$ mice. One to two days later, the contralateral retinae of these mice were isolated and quantitatively analyzed for labeled RGCs ([A and B], wild-type; [C and D], *EphA7*$^{-/-}$; see Experimental Procedures). The location of individual labeled cells was recorded, as shown in the smaller retinal panels. The injection sites for (A) and (C) were smaller (2.0% and 2.0% of SC, respectively) than for (B) and (D) (4.5% and 3.1% of SC, respectively). The larger retinal panels show the 5% and 20% peak density contour lines delineating those parts of the retina having a density of labeled cells greater than 5% (or 20%) of the maximum density of labeled cells. This analysis was based on the numbers of cells recorded within a sample box at different grid locations. Both the raw distributions and the isodensity contours uncovered ectopic foci in the nasal part of the retinae of *EphA7*$^{-/-}$ mutant mice (C and D), while none were found in wild-type mice (A and B). In addition, in *EphA7*$^{-/-}$ mice, the 20% and 5% peak density contour lines of the foci of temporal axons were enlarged, indicating increased TZs of temporal axons in *EphA7*$^{-/-}$ mice. Corresponding sections from the SC of wild-type and *EphA7*$^{-/-}$ mice with their injection sites in the anterior SC are shown in (E) and (F), respectively. There are no obvious differences in the size of the SC of wild-type and mutant mice. Anterior and posterior borders of the SC are indicated by arrows. A, anterior; D, dorsal; P, posterior; V, ventral.

tracings suggest that temporal axons form more extended TZs in *EphA7*$^{-/-}$ than in wild-type mice.

EphA7 Repels Retinal Axons in Stripe Assay Experiments

The projection of nasal axons with a higher ephrin-A expression onto the posterior SC with a lower EphA expression, and vice versa, suggests a repellent function of EphA7 as the mechanism by which this "ligand" contributes to the guidance of retinal axons in the SC. To further approach this concept and to better understand the mechanism(s) causing the formation of eTZs in *EphA7*$^{-/-}$ mice, we took advantage of the stripe assay technique (Hornberger et al., 1999; Knöll et al., 2001; Vielmetter et al., 1990). Alternating lanes of EphA7-Fc versus Fc were produced on plastic dishes and covered with laminin (see Experimental Procedures). Then strips from mouse E15.5–16.5 or chick E7 retinae were arranged perpendicular to these lanes, and the outgrowth preferences of retinal axons were scored 2 days later. Growth preferences were evaluated according to the scoring system of Walter et al. (1987), with 3 indicating a very strong preference and 0 indicating no preference at all. It was thought likely that chick retinal axons would behave in a comparable way to mouse retinal axons, since overall ephrin-A and EphA expression patterns are conserved in the chick and mouse retinotectal/collicular projection (Figure 1; data not shown; Connor et al., 1998; Feldheim et al., 2000; Hornberger et al., 1999; Marcus et al., 1996; Takahashi et al., 2003).

When given the choice of growing on alternating EphA7-Fc- versus Fc-containing stripes, both chick (mean score 1.5 ± 0.11, n = 31) and mouse (mean score 2.2 ± 0.22, n = 16) retinal axons showed a preference for Fc stripes (Figures 7A and 7E), suggesting that retinal axons were repelled from growing on EphA7-Fc stripes. In control stripe assays with Fc/Fc lanes (Figures 7B and 7F), retinal axons essentially showed unpatterned outgrowth (chick: mean score 0.27 ± 0.09, n = 29; mouse: 0.96 ± 0.27, n = 9). Thus, although ex-

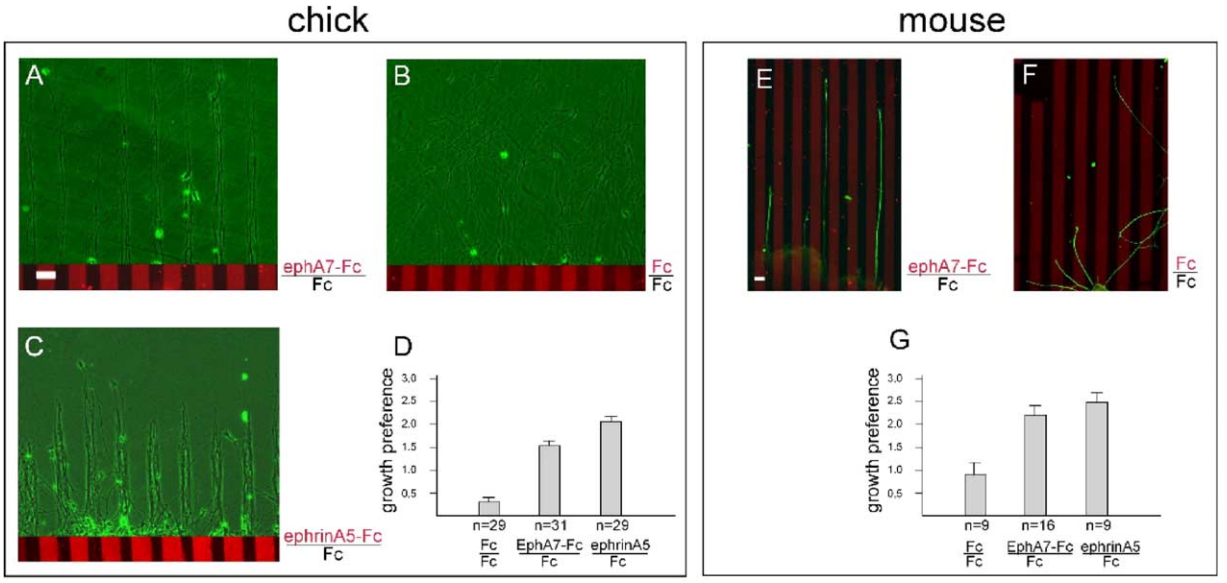

Figure 7. Analysis of EphA7 "Ligand" Function in Stripe Assay Experiments

(A–D) Stripe assay data using E7 chick retinae; (E–G) stripe assay data using E15.5–E16.5 mouse retinae. (A and E) When grown on a substrate of alternating lanes of EphA7-Fc and Fc, chick retinal axons showed a preference for Fc-containing lanes, indicating a repulsion from growing on EphA7-Fc stripes. (B and F) On a control substrate of alternating Fc and Fc stripes, retinal axons did not show any, or only a slight preference. (C) On a substrate of alternating lanes of ephrin-A5-Fc and Fc, retinal axons showed a preference for Fc stripes. (D and G) Summary of four (chick) or two (mouse) independently performed experiments, with the total number of retinal strips analyzed (n) given below the bars. Growth preferences were evaluated according to the scoring system of Walter et al. (1987), with 3 indicating a very strong preference and 0 indicating no preference at all. Mouse retinal axons typically show a stronger level of fasciculation than chick retinal axons (see also Feldheim et al., 2000). In all cases shown, nasal retina is to the left, temporal retina to the right. Additional control stripe assay experiments performed in the presence of soluble EphA7-Fc are shown in Figure S2. After preparing the stripes, laminin was added to provide an outgrowth-promoting substrate for retinal axons. Identification of the individual stripes was achieved by adding small amounts of Cy3-labeled antibody to the stripes generated first (see Experimental Procedures). Thus, under TRITC illumination, as shown in the lower panels in (A)–(C), first generated stripes can be discriminated from second generated stripes. (E) and (F) represent overlays of pictures taken from tubulin-stained axons and the Cy3-labeled stripes. Bars shown in (A) and (E) correspond to 90 μm. Error bars represent SEM.

pressing ephrin-As at different levels, nasal and temporal axons showed a preference for Fc stripes, possibly relating to the amounts of EphA7-Fc used to generate the stripes (see also Discussion).

To further investigate the role of EphA7-Fc in this striped outgrowth pattern, we performed experiments in which we added soluble, clustered EphA7-Fc at 1 μg/ml to the medium. Here the growth decision was almost completely abolished, while incubation with clustered Fc alone had no effect (see Figure S2). These data indicate, first, that interfering specifically with ephrin-A→EphA interactions results in an abolishment of the patterned outgrowth of retinal axons, and, second, that the striped outgrowth is due to a repulsion of retinal axons from growing on EphA7-Fc-containing lanes and not to an attractive effect of Fc-containing lanes.

In an attempt to compare the strength of repulsion mediated by EphA7-Fc (reverse signaling) to that of ephrin-A5-Fc (forward signaling), stripe assay experiments were performed using ephrin-A5-Fc versus Fc. Due to technical reasons it is not possible to compare directly the activities of ephrin-A5 and EphA7, as during set-up of such a striped substrate these Fc proteins would bind and block each other.

In the experiments shown in Figures 7C and 7G, ephrin-A5-Fc stripes led to a stronger repulsion of both chick (2.0 ± 0.12, n = 29) and mouse (2.5 ± 0.21, n = 9) retinal axons compared to that on EphA7-Fc/Fc stripes (Figures 7D and 7G). Further analysis of the growth preference showed that the mean score for Fc/Fc control stripe assays was statistically significantly lower than that for EphA7-Fc/Fc ($p < 0.05$; t test) and ephrin-A5-Fc/Fc stripe assays ($p < 0.05$, t test). It appears therefore that forward signaling has a stronger repellent activity on retinal axons than reverse signaling. However, this finding cannot be generalized, given the rather artificial conditions here in the stripe assay, such as the use of Fc fusion proteins.

Discussion

Topographic Mapping by Interstitial Branching

In mouse (and chick), retinal axons grow into the SC in a nontopographic manner and significantly overshoot their future TZs (Simon and O'Leary, 1992; Yates et al., 2001). In a subsequent step, branching and arborization occurs ab initio with high topographic specificity, which is further refined during later development (Yates et al., 2001). Thus, it appears that the primary growth cone is not directly involved in determining the correct location of the future TZ, but is formed through intersti-

tial branching from the axon shaft (Yates et al., 2001; as a possible mechanism for branch induction, see Davenport et al., 1999).

Recent experiments by Yates et al. (2001) have provided evidence that suppression of branching posterior to future TZs is controlled through the repellent activity of ephrin-As acting on EphA receptor-expressing retinal axons. However, as this EphA^{retina}/ephrin^{SC} system can control branching only on one side of a TZ, a countergradient system appears to be necessary to regulate branching anterior to future TZs in order to achieve a confined branching zone (Figure 1A; Yates et al., 2004; Yates et al., 2001).

The differential expression of ephrin-As on retinal axons and of EphA receptors in the SC in countergradients to the EphA^{retina}/ephrin-A^{SC} expression pattern (Figure 1B) makes them good candidates for exerting this activity. Thus, ephrin-As are expressed more strongly on nasal than temporal axons (Figure 3; Hornberger et al., 1999; Marcus et al., 1996), while the EphA7 receptor shows an anterior > posterior expression in the superficial retinorecipient layers of the SC and is not expressed on retinal axons (Figures 2 and 4). This configuration of the gradients in particular would be well suited to mediate branch suppression anterior to developing TZs. It would mean that the higher the expression of ephrin-As is on retinal axons, the further posterior the TZ is formed. In consequence, in the absence of EphA7, (additional) TZs would form in the more anterior SC.

Topographic Mapping Defects in *EphA7*$^{-/-}$ Mice

In support of this model, we found—using anterograde and retrograde tracing techniques—mapping defects for both nasal and temporal axons.

On the one hand, nasal axons formed eTZs in the anterior SC of *EphA7*$^{-/-}$ mice (Figures 5 and 8). The penetrance of these mapping defects—about 60% in both studies—is comparable to that of other EphA family mutants (Feldheim et al., 2000; Frisen et al., 1998). It is not clear at present why the eTZs from nasal axons form in the more anterior part of the SC and not, as possibly more expected, close(r) to the correct TZ in the posterior SC. However, the eTZs are formed *anterior* to the correct TZs, which correlates well with the model described in Figure 1. Other EphA receptors such as EphA3, which also is expressed in a gradient in the SC (Figure 2C), could be involved in the control of mapping too. In addition, the generally moderate penetrance of EphA family knockouts suggests the involvement of additional guidance systems in the retinocollicular projection beyond that provided by the Eph family.

On the other hand, mapping errors were found also for temporal axons. A quantification of data derived from retrograde tracing experiments showed a larger than normal area of labeled RGCs following the injection of fluorescent beads into the anterior quarter of the SC from *EphA7*$^{-/-}$ mice, indicating in turn more extended TZs of temporal axons (Figures 6 and 8). As temporal (as well as nasal) retinal axons are repelled in the stripe assay from growing on EphA7-Fc lanes (Figure 7; see below), it appears plausible to assume that this defect is a *direct* consequence of the lack of EphA7 in the SC of *EphA7*$^{-/-}$ mice. A delay in the development of the SC as a cause for this defect can be excluded, as the experiments were performed at least 1 week after maturation of the map. However, we cannot exclude that (part of) the effects are due to an increased competition between temporal axons and aberrantly projecting nasal axons.

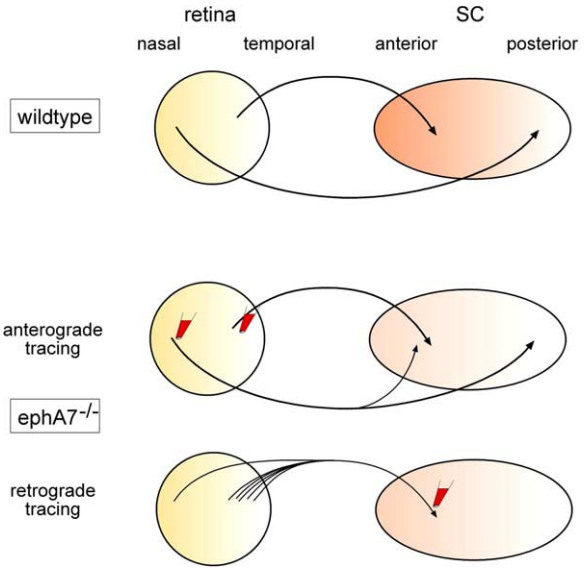

Figure 8. Topographic Targeting Defects of Nasal Retinal Axons in *EphA7*$^{-/-}$ Mice

In wild-type mice, temporal and nasal axons project onto the anterior and posterior SC, respectively. The gradients of ephrin-As and EphAs in retina and SC, respectively, are indicated (see also Figure 1). *EphA7*$^{-/-}$ mice have been analyzed by both anterograde and retrograde tracing techniques. Anterograde tracing showed a projection of temporal axons onto the anterior SC, while nasal axons projected onto the posterior SC and aberrantly onto the anterior SC. A disturbed projection pattern is seen also in retrograde tracing experiments, in which injection of fluorescent microspheres into the anterior SC resulted in the labeling of RGCs in both nasal and temporal retina, indicating that temporal and aberrantly nasal axons project onto the anterior SC in *EphA7*$^{-/-}$ mice. In addition, the area of labeled RGCs in the temporal retina was significantly enlarged in *EphA7*$^{-/-}$ mice, suggesting that temporal axons form more extended TZs in the anterior SC.

The enlarged foci in *EphA7*$^{-/-}$ mice were not readily apparent in anterograde tracings. In this type of experiment it was more difficult, due to technical reasons, to control the amount of DiI injected into the retinae, which per se led to some variation in the size of TZs in wild-type and mutant mice.

Interestingly, during development of, for example, the zebrafish retinotectal projection, retinal axons are guided directly to their TZs without a "branching intermediate" (Stuermer, 1988). Nevertheless, countergradients of EphAs and ephrin-As are present in the zebrafish tectum and retina (e.g., Brennan et al., 1997). Thus, these gradients may not be merely a reflection of necessities of a branching mechanism, but may be required to provide retinal axons in general with sufficient positional information to find their target area, in agreement with the

proposal originally formulated by Gierer (Gierer, 1983, 1988; see Introduction).

In direct support of our experimental data, a computational model of map development has been designed, which shows that countergradients of EphAs and ephrin-As in both the retina and the SC, and bidirectional repellent signaling between retinal axons and SC cells, are sufficient to direct a topographic bias in retinal axon branching (Yates et al., 2004).

Recently it has been shown that ephrin-As in their ligand function do not only exert repellent, but also outgrowth promoting/attractant effects on retinal axons (Hansen et al., 2004). These effects were concentration dependent and were different for axons from different retinal positions. These findings have led to a mapping model in which ephrin-As act as topographic labels that promote axon growth at lower concentrations while suppressing growth at higher concentrations. Similar principles might apply to the function of EphAs in the SC uncovered in this investigation. Moreover, such a dual function might hold true not only for primary growth cone behavior but also for branching processes (see also below). Thus, the study by Hansen et al. (2004) and data presented in this investigation do support the same idea that the EphA/ephrin-A guidance system provides a countergradient scheme as proposed by Gierer (1983, 1988).

Stripe Assay Experiments

Stripe assay experiments were performed to obtain a first idea of the mechanism(s) by which EphA7 might exert its ligand function in the SC. We found in these experiments that both chick and mouse retinal axons were repelled from growing on EphA7-Fc-containing stripes (Figure 7). The lack of an obvious differential sensitivity of nasal versus temporal axons toward EphA7 could be due to the fact that ephrin-As are indeed expressed on both classes of axons—though at different levels. Thus, the elevated EphA7 concentrations used in the stripe assay experiments possibly result in a significant activation of ephrin-As on both nasal and temporal axons and an avoidance to growing on EphA7-containing stripes. Alternatively, the appearance of a differential sensitivity of nasal versus temporal axons in this axon guidance assay might require additional cofactors that are not present under these conditions. However, these in vitro data are consistent with our in vivo data, as the mapping of both nasal and temporal axons was also affected here.

Recent analyses of the EphA^{retina}/ephrin-A^{SC} module indicate that in this case axon guidance and branching are closely linked (see Introduction; Yates et al., 2001). This appears to be true also for other axon guidance families, such as Slit-2, a ligand for Robo axon guidance receptors, which mediates both repulsion and branching (Brose and Tessier-Lavigne, 2000; Wang et al., 1999; see also Heffner et al., 1990; Ng et al., 2002; Thies and Davenport, 2003). Thus, repulsion of retinal axons from growing on EphA7-Fc-containing lanes might well correspond to an EphA7-mediated suppression of branching of retinal axons in the SC. It would then be expected that guidance and branching are sensitive to different thresholds of EphA/ephrin-A activation. Thus, the primary growth cone would be less sensitive to ephrin-As than the axon shaft and would advance further ahead at concentrations of ephrin-As, which would suppress branching.

Interestingly, retinal axons invade the SC from the high end of the repellent EphA7 gradient, which is already present at the time of ingrowth of retinal axons into the SC. Possibly, retinal axons are initially insensitive to the repellent activity of EphA7 (perhaps because ephrin-As are not exposed at the surface of retinal growth cones) and turn sensitive only upon a particular signal, the nature of which is not known at present. Such a change in sensitivity might be developmentally controlled and/or might be induced when retinal axons approach the posterior end of the SC. In fact, earlier investigations have shown that retinal axons can enter the tectum at quite different positions—e.g., from the posterior tectum—and still find their correct target area (Fujisawa, 1981), suggesting that retinal axons are well able to enter the target area from the high end of an EphA/ephrin-A gradient, can grow "downhill" an ephrin-A or an EphA gradient, and still finding their correct target. Additionally, in vitro experiments have shown that retinal axons can surmount a step gradient of repellent material when confronted with it at a right angle to its growth direction but are more likely deflected when hitting the step gradient at a shallow angle (T.R. and U.D., unpublished data).

Previous Characterisations of Retinal Ephrin-A Expression

It has been shown previously (Dütting et al., 1999; Hornberger et al., 1999) that a modulation of the level of retinal ephrin-A expression results in a change in the sensitivity of these axons toward guidance cues in the tectum. These data correlate well with the data derived from the characterization of *EphA7*$^{-/-}$ mice presented here. One of the possible interpretations given earlier to explain these data was that ephrin-As on retinal axons could possibly modify the function of coexpressed EphA receptors, thus acting as an ephrin-A^{retina}/EphA^{retina} module (Hornberger et al., 1999; McLaughlin and O'Leary, 1999). In fact, one important aspect of the complex EphA/ephrin-A interactions in retinotectal/collicular mapping appears to be an unusual *cis*-interaction between EphAs and ephrin-As within the same membrane (the EphA^{retina}/ephrin-A^{retina} module), leading to a modulation of EphA receptor function (R. Carvalho and U.D., unpublished data). However, the analysis of *EphA7*$^{-/-}$ mice presented here now exposes an additional aspect controlling retinocollicular mapping, which is the involvement of an ephrin-A^{retina}/EphA^{SC} module.

The ability to function as receptors (reverse signaling) was recognized initially for the transmembrane-anchored ephrin-Bs (Brückner et al., 1997; Holland et al., 1996), while experimental evidence for such a function of the GPI-anchored ephrin-As has emerged only later (Davy et al., 1999; Davy and Robbins, 2000; Huai and Drescher, 2001; Knöll et al., 2001).

In the vomeronasal system, for example, axonally expressed ephrin-As mediate an "attractive" function fitting with their projection into a region of the AOB with

high(er) EphA expression (Knöll et al., 2001). In the retinocollicular projection, however, in vivo and in vitro data suggest a repulsive interaction, which in turn correlates well with their expression patterns, as nasal axons with a high(er) ephrin-A expression project onto the area of the SC with a low(er) EphA expression (and vice versa). There is at present no indication of which factors determine ephrin-A-mediated attraction versus repulsion; however, it might be possible that different signal-transducing ephrin-A coreceptor(s) are expressed on vomeronasal and retinal axons.

Experimental Procedures

In Situ Hybridization

Mouse ephrin-A and EphA probes used have been described previously (Knöll et al., 2001). In situ hybridization was performed according to the protocol of Wilkinson and Nieto (1993) using digoxygenin-labeled probes.

Targeted Disruption of the EphA7 Gene

For homologous recombination, 5′ EcoRI-XhoI 3 kb sequence and 3′ NotI-SalI 5.3 kb sequence flanking exon I (1–330 bp of the EphA7 cDNA), including part of the upstream sequence (–601 to –1), were subcloned into pBluescript vector (Figure 4). A loxP-flanked tk/neo selection cassette containing a neomycin-resistance gene (*neo*) and the thymidine kinase gene, both with the phosphoglycerate (*pgk*) promoter and *pgk* polyadenylation signal, was cloned between these genomic sequences. The R1 embryonic stem cell line was electroporated with the linearized targeting construct and selected with G418 for 10 days. A total of 360 surviving clones were expanded, and homologous recombinants were identified by Southern blot analysis of genomic DNA from single clones digested with EcoRI. The 5′ end of the targeted allele was checked for integrity using 5′-CTTGACAGCTAAATATCTGGATAAAGAGATC-3′ sense and 5′-CATTACACTTCCAGACCTGGGAC-3′ reverse primer generating a 3.6 kb band in case of correct homologous recombination. From the 12 resulting positive clones, three were transfected with expression plasmid pIC-Cre coding for Cre recombinase in order to remove the loxP-flanked tk/neo selection cassette. Clones were counterselected with the thymidine kinase substrate gancyclovir (2 μM). Surviving clones were expanded and tested with the genomic probe as described above. To prove the correct removal of the loxP-flanked tk/neo selection cassette, genomic DNA was tested in a PCR reaction using 5′-CTAAGGTCCTATTTTGCCTG-3′ sense primer and the reverse primer described above, leading to the amplification of a 0.5 kb band from the targeted allele.

Chimeras were mated to C57BL/6 mice to produce heterozygotes. Southern blot analysis and PCR analysis were used for genotyping the offspring. Primers used in RT-PCR for demonstrating the absence of the signal peptide of EphA7 in transgenic animals were 5′-GTCTGCAGTCGGAGACTTGCAG-3′ and 5′-CTTCGCAG CCTGCGCCTC-3′, amplifying a 314 bp band from the 5′ region of the EphA7 mRNA.

Ephrin-A Staining on Mouse Retinal Axons

Nasal or temporal retinal explants taken from E14.5 mouse embryos were grown in neurobasal medium plus B27 supplement for 2 days on poly-L-Lysine and Laminin-coated cover slips. Explants were incubated with 5 μg/ml EphA7-Fc (R&D Systems) or Fc alone (Calbiochem) in neurobasal medium for 30 min at 37°C. After washing with PBS, explants were fixed with 4% PFA/PBS for 15 min at room temperature and washed again with PBS. Bound EphA7-Fc or Fc protein was visualized with a goat anti-human Fc Cy3-conjugated antibody (Sigma, 1:200) for 1 hr in 2% BSA/PBS. Following additional washing steps with PBS, explants were mounted in moviol and analyzed using a Zeiss Axiovert M200 and a 40× objective.

In Vivo Analysis of Retinotopic Mapping

Anterograde Labeling

EphA7$^{-/-}$ mice and wild-type littermates were analyzed at P10–P14. Mice were anesthetised with a combination of Hypnorm and Hypnovel, and anterograde tracing of retinal axons was performed by focal injection of DiI (Molecular Probes, Eugene, OR) as a 10% solution in either ethanol or dimethylformamide into the peripheral region of dorsotemporal or ventronasal retina, following the protocol of Simon and O'Leary (1992). Briefly, DiI was pressure injected with a Picospritzer II (General Valve) through a glass micropipette (internal diameter of tip ~50 μm). The DiI-labeled area usually covered less than 5% of the retina. About 24–48 hr later, the mice were deeply anesthetized and perfused transcardially with 4% paraformaldehyde. Before its removal, incisions were made into the retina to be able to determine later the topographic position of the DiI spot. The SC and IC as well as the injected retinae were whole mounted onto glass slides and examined under UV light. The injection sites of all retinae were verified by fluorescence imaging of flat mounts. There was no difference in size or location of retinal injections or general structure of the retina between wild-type and mutant littermates that could be responsible for the altered projections observed in *EphA7*$^{-/-}$ mice. TZs were verified by their branched appearance at high magnification.

Retrograde Labeling

Under anesthesia, a small craniotomy was made in P14–P18 mice over the right SC. Injection of 20 nl of red or green fluorescent latex microspheres (Lumafluor Inc., FL), diluted 1 in 5 with distilled water, was made in the superficial layers of the SC through a glass micropipette (10–20 μm tip diameter) using air pressure. Once recovered, mice were returned to their mothers for 24–48 hr. Then animals were terminally anesthetized with sodium pentobarbitone and perfused transcardially with PBS followed by 1% PFA in 0.1 M phosphate buffer (PB). The eyes were removed after making a knife mark in the superior cornea to orient the eye, and perfusion was continued with 4% PFA in PB. Retinae were dissected out of the eyes, flat mounted on glass slides, and postfixed in 4% PFA overnight before they were dried and cover slipped using Hydromount (Natural Diagnostics Ltd, East Riding, UK). To check the injection site, brains were postfixed in 4% PFA overnight, cryoprotected in 30% sucrose in PB, and then sectioned parasagittally at 50 μm on a freezing microtome. One in two sections was mounted on gelatinized slides and coverslipped with Hydromount for analysis of the injection site. A second series was Nissl stained for identification of anatomical structures.

Data Collection and Analysis

The retinal locations of RGCs containing fluorescent microspheres were digitally recorded using a camera lucida setup and inhouse software. The software recorded the retinal outline, the x, y location of each cell, and also the number of cells within the sample square at each grid location. The outline of the retina was plotted at low magnification, and the location of labeled cells were recorded at high magnification. In general, the whole retina was sampled in a one in four series of 200 × 200 μm sample boxes in a 200 × 200 μm grid. In areas of higher numbers of labeled cells (temporal focus and ectopic nasal foci), every grid point was sampled within the focus. For determination of the size of foci, the data were analyzed using SYSTAT Statistics software (Evanston, IL), which calculates isodensity lines of labeling for each retina. Contour analysis was done using the sample grid locations and the numbers of cells in each sample square. Smoothing was done using distance-weighted least-squares smoothing and employing the default tensions in the program. The areas enclosed by the 20% and 5% contour lines (representing densities at 20% or 5% of the peak density, i.e., the maximum number of cells in a sample square) were expressed as a percentage of the total retinal area. The percentage area of the SC covered by each injection site was calculated from a series of parasagittal sections. The outline of the SC was determined from a Nissl-stained series of sections; the extent of the injection site was measured under fluorescent illumination in the Hydromount-covered sections. The relative injection site area was calculated by measuring the rostrocaudal extent of the superior colliculus and the spread of beads in every second 50 μm section through the entire mediolateral extent of the right SC.

Stripe Assay

A modified version of the stripe assay (Vielmetter et al., 1990) was performed using essentially the protocol described by Hornberger

et al. (1999). However, here we used 30 μg/ml Fc, EphA7-Fc, or ephrin-A5-Fc (all unclustered) for generation of the first stripe, and also 30 μg/ml Fc for generation of the second stripe. Laminin concentrations used were 20 μg/ml. To allow a discrimination between first and second stripe during subsequent analysis of retinal outgrowth preferences and to judge the quality of striped "carpets," proteins from the first stripe were mixed with 2 μg/ml Cy3-labeled anti-human Fc antibody, while Fc protein was incubated with the same concentration of the same, but unlabeled, anti human-Fc antibody.

In total, four independent experiments were performed with chick retinal axons, with in each case at least eight retinal stripes for each condition (EphA7-Fc/Fc, ephrin-A5-Fc/Fc, or Fc/Fc). Similarly, for mouse retinal axons, two independent experiments were performed. In all experiments, EphA7-Fc/Fc and ephrin-A5-Fc/Fc stripe assays were unambiguously discriminated from Fc/Fc stripe assays.

Supplemental Data

The Supplemental Data for this article can be found online at http://www.neuron.org/cgi/content/full/47/1/57/DC1/.

Acknowledgments

This work was supported by the Wellcome Trust. We are grateful to Sarah Guthrie, Guy Tear, Franco Weth, Elena Becker, Ricardo Carvalho, Richard Wingate, and Rosemary Drescher for critical comments on the manuscript.

Received: June 16, 2004
Revised: January 27, 2005
Accepted: May 26, 2005
Published: July 6, 2005

References

Brennan, C., Monschau, B., Lindberg, R., Guthrie, B., Drescher, U., Bonhoeffer, F., and Holder, N. (1997). Two Eph receptor tyrosine kinase ligands control axon growth and may be involved in the creation of the retinotectal map in the zebrafish. Development *124*, 655–664.

Brose, K., and Tessier-Lavigne, M. (2000). Slit proteins: key regulators of axon guidance, axonal branching, and cell migration. Curr. Opin. Neurobiol. *10*, 95–102.

Brown, A., Yates, P.A., Burrola, P., Ortuno, D., Vaidya, A., Jessell, T.M., Pfaff, S.L., O'Leary, D.D., and Lemke, G. (2000). Topographic mapping from the retina to the midbrain is controlled by relative but not absolute levels of EphA receptor signaling. Cell *102*, 77–88.

Brückner, K., Pasquale, E.B., and Klein, R. (1997). Tyrosine phosphorylation of transmembrane ligands for Eph receptors. Science *275*, 1640–1643.

Ciossek, T., Millauer, B., and Ullrich, A. (1995). Identification of alternatively spliced mRNAs encoding variants of MDK1, a novel receptor tyrosine kinase expressed in the murine nervous system. Oncogene *10*, 97–108.

Cohen-Cory, S. (1999). BDNF modulates, but does not mediate, activity-dependent branching and remodeling of optic axon arbors in vivo. J. Neurosci. *19*, 9996–10003.

Cohen-Cory, S., and Fraser, S.E. (1995). Effects of brain-derived neurotrophic factor on optic axon branching and remodelling in vivo. Nature *378*, 192–196.

Connor, R.J., Menzel, P., and Pasquale, E.B. (1998). Expression and tyrosine phosphorylation of Eph receptors suggest multiple mechanisms in patterning of the visual system. Dev. Biol. *193*, 21–35.

Conover, J.C., Doetsch, F., Garcia-Verdugo, J.M., Gale, N.W., Yancopoulos, G.D., and Alvarez-Buylla, A. (2000). Disruption of Eph/ephrin signaling affects migration and proliferation in the adult subventricular zone. Nat. Neurosci. *3*, 1091–1097.

Davenport, R.W., Thies, E., and Cohen, M.L. (1999). Neuronal growth cone collapse triggers lateral extensions along trailing axons. Nat. Neurosci. *2*, 254–259.

Davy, A., and Robbins, S.M. (2000). EphrinA5 modulates cell adhesion and morphology in an integrin-dependent manner. EMBO J. *19*, 5396–5405.

Davy, A., Gale, N.W., Murray, E.W., Klinghofer, R.A., Soriano, P., Feuerstein, C., and Robbins, S.M. (1999). Compartmentalized signaling by GPI-anchored ephrinA5 requires the fyn tyrosine kinase to regulate cellular adhesion. Genes Dev. *13*, 3125–3135.

Debski, E.A., and Cline, H.T. (2002). Activity-dependent mapping in the retinotectal projection. Curr. Opin. Neurobiol. *12*, 93–99.

Dütting, D., Handwerker, C., and Drescher, U. (1999). Topographic targeting and pathfinding errors of retinal axons following overexpression of ephrinA ligands on retinal ganglion cell axons. Dev. Biol. *216*, 297–311.

Feldheim, D.A., Vanderhaeghen, P., Hansen, M.J., Frisen, J., Lu, Q., Barbacid, M., and Flanagan, J.G. (1998). Topographic guidance labels in a sensory map to the forebrain. Neuron *21*, 1303–1313.

Feldheim, J., Kim, Y.-I., Bergemann, A.D., Frisén, J., Barbacid, M., and Flanagan, J.G. (2000). Genetic analysis of ephrin-A2 and ephrin-A5 shows their requirement in multiple aspects of retinocollicular mapping. Neuron *25*, 563–574.

Feldheim, D.A., Nakamoto, M., Osterfield, M., Gale, N.W., DeChiara, T.M., Rohatgi, R., Yancopoulos, G.D., and Flanagan, J.G. (2004). Loss-of-function analysis of EphA receptors in retinotectal mapping. J. Neurosci. *24*, 2542–2550.

Frisen, J., Yates, P.A., McLaughlin, T., Friedman, G.C., O'Leary, D.D.M., and Barbacid, M. (1998). Ephrin-A5 (AL-1/RAGS) is essential for proper retinal axon guidance and topographic mapping in the mammalian visual system. Neuron *20*, 235–243.

Fujisawa, H. (1981). Retinotopic analysis of fiber pathways in the regenerating retinotectal system of the adult newt cynops Pyrrhogaster. Brain Res. *206*, 27–37.

Gierer, A. (1983). Model for the retinotectal projection. Proc. R Soc. Lond. B Biol. Sci. *218*, 77–93.

Gierer, A. (1988). Spatial organization and genetic information in brain development. Biol. Cybern. *59*, 13–21.

Goodhill, G.J. (2000). Dating behavior of the retinal ganglion cell. Neuron *25*, 501–503.

Goodhill, G.J., and Richards, L.J. (1999). Retinotectal maps: molecules, models and misplaced data. Trends Neurosci. *22*, 529–534.

Hansen, M.J., Dallal, G.E., and Flanagan, J.G. (2004). Retinal axon response to ephrinAs shows a graded, concentration-dependent transition from growth promotion to inhibition. Neuron *42*, 717–730.

Heffner, C.D., Lumsden, A.G., and O'Leary, D.D. (1990). Target control of collateral extension and directional axon growth in the mammalian brain. Science *247*, 217–220.

Hindges, R., McLaughlin, T., Genoud, N., Henkemeyer, M., and O'Leary, D.D. (2002). EphB forward signaling controls directional branch extension and arborization required for dorsal-ventral retinotopic mapping. Neuron *35*, 475–487.

Holland, S.J., Gale, N.W., Mbamalu, G., Yancopoulos, G.D., Henkemeyer, M., and Pawson, T. (1996). Bidirectional signalling through the eph-family receptor Nuk and its transmembrane ligands. Nature *383*, 722–725.

Hornberger, M.R., Dutting, D., Ciossek, T., Yamada, T., Handwerker, C., Lang, S., Weth, F., Huf, J., Wessel, R., Logan, C., et al. (1999). Modulation of EphA receptor function by coexpressed ephrinA ligands on retinal ganglion cell axons. Neuron *22*, 731–742.

Huai, J., and Drescher, U. (2001). An ephrinA-dependent signaling pathway controls integrin function and is linked to the tyrosine phosphorylation of a 120 kDa protein. J. Biol. Chem. *276*, 6689–6694.

Katz, L.C., and Shatz, C.J. (1996). Synaptic activity and the construction of cortical circuits. Science *274*, 1133–1138.

Knöll, B., and Drescher, U. (2002). Ephrin-As as receptors in topographic projections. Trends Neurosci. *25*, 145–149.

Knöll, B., Zarbalis, Z., Wurst, W., and Drescher, U. (2001). A role for

the EphA family in the topographic targeting of vomeronasal axons. Development *128*, 895–906.

Kullander, K., and Klein, R. (2002). Mechanisms and functions of eph and ephrin signalling. Nat. Rev. Mol. Cell Biol. *3*, 475–486.

Loschinger, J., Weth, F., and Bonhoeffer, F. (2000). Reading of concentration gradients by axonal growth cones. Philos. Trans. R. Soc. Lond. B Biol. Sci. *355*, 971–982.

Mackarehtschian, K., Lau, C.K., Caras, I., and McConnell, S.K. (1999). Regional differences in the developing cerebral cortex revealed by ephrin-A5 expression. Cereb. Cortex *9*, 601–610.

Marcus, R.C., Gale, N.W., Morrison, M.E., Mason, C.A., and Yancopoulos, G.D. (1996). Eph family receptors and their ligands distribute in opposing gradients in the developing mouse retina. Dev. Biol. *180*, 786–789.

Marin, O., Blanco, M.J., and Nieto, M.A. (2001). Differential expression of eph receptors and ephrins correlates with the formation of topographic projections in primary and secondary visual circuits of the embryonic chick forebrain. Dev. Biol. *234*, 289–303.

McLaughlin, T., and O'Leary, D.D.M. (1999). Functional consequences of coincident expression of EphA receptors and ephrinA ligands. Neuron *22*, 636–639.

McLaughlin, T., Torborg, C.L., Feller, M.B., and O'Leary, D.D. (2003a). Retinotopic map refinement requires spontaneous retinal waves during a brief critical period of development. Neuron *40*, 1147–1160.

McLaughlin, T., Hindges, R., and O'Leary, D.D. (2003b). Regulation of axial patterning of the retina and its topographic mapping in the brain. Curr. Opin. Neurobiol. *13*, 57–69.

Nakamura, H., and O'Leary, D.D.M. (1989). Inaccuracies in initial growth and arborization of chick retinotectal axons followed by course corrections and axon remodeling to develop retinotectal order. J. Neurosci. *9*, 3776–3795.

Ng, J., Nardine, T., Harms, M., Tzu, J., Goldstein, A., Sun, Y., Dietzl, G., Dickson, B.J., and Luo, L. (2002). Rac GTPases control axon growth, guidance and branching. Nature *416*, 442–447.

Park, S., Frisen, J., and Barbacid, M. (1997). Aberrant axonal projections in mice lacking EphA8 (Eek) tyrosine kinase receptors. EMBO J. *16*, 3106–3114.

Reber, M., Burrola, P., and Lemke, G. (2004). A relative signalling model for the formation of a topographic neural map. Nature *431*, 847–853.

Roskies, A.L., and O'Leary, D.D.M. (1994). Control of topographic retinal axon branching by inhibitory membrane-bound molecules. Science *265*, 799–803.

Simon, D.K., and O'Leary, D.D.M. (1992). Development of topographic order in the mammalian retinocollicular projection. J. Neurosci. *12*, 1212–1232.

Sperry, R.W. (1963). Chemoaffinity in the orderly growth of nerve fiber patters and connections. Proc. Natl. Acad. Sci. USA *50*, 703–710.

Stuermer, C.A. (1988). Retinotopic organization of the developing retinotectal projection in the zebrafish embryo. J. Neurosci. *8*, 4513–4530.

Takahashi, H., Shintani, T., Sakuta, H., and Noda, M. (2003). CBF1 controls the retinotectal topographical map along the anteroposterior axis through multiple mechanisms. Development *130*, 5203–5215.

Thies, E., and Davenport, R.W. (2003). Independent roles of Rho-GTPases in growth cone and axonal behavior. J. Neurobiol. *54*, 358–369.

Vielmetter, J., Stolze, B., Bonhoeffer, F., and Stuermer, C.A. (1990). In vitro assay to test differential substrate affinities of growing axons and migratory cells. Exp. Brain Res. *81*, 283–287.

Walter, J., Henke-Fahle, S., and Bonhoeffer, F. (1987). Avoidance of posterior tectal membranes by temporal retinal axons. Development *101*, 909–913.

Wang, K.H., Brose, K., Arnott, D., Kidd, T., Goodman, C.S., Henzel, W., and Tessier-Lavigne, M. (1999). Biochemical purification of a mammalian slit protein as a positive regulator of sensory axon elongation and branching. Cell *96*, 771–784.

Wilkinson, D.G. (2000). Topographic mapping: organising by repulsion and competition? Curr. Biol. *10*, R447–R451.

Wilkinson, D.G., and Nieto, M.A. (1993). Detection of messenger RNA by in situ hybridization to tissue sections and whole mounts. Methods Enzymol. *225*, 361–373.

Willshaw, D.J., and von der Malsburg, C. (1976). How patterned neural connections can be set up by self-organization. Proc R Soc. Lond. B Biol. Sci. *194*, 431–445.

Yates, P.A., Roskies, A.L., McLaughlin, T., and O'Leary, D.D. (2001). Topographic-specific axon branching controlled by ephrin-as is the critical event in retinotectal map development. J. Neurosci. *21*, 8548–8563.

Yates, P.A., Holub, A.D., McLaughlin, T., Sejnowski, T.J., and O'Leary, D.D. (2004). Computational modeling of retinotopic map development to define contributions of EphA-ephrinA gradients, axon-axon interactions, and patterned activity. J. Neurobiol. *59*, 95–113.

Yun, M.E., Johnson, R.R., Antic, A., and Donoghue, M.J. (2003). EphA family gene expression in the developing mouse neocortex: regional patterns reveal intrinsic programs and extrinsic influence. J. Comp. Neurol. *456*, 203–216.

Zhou, R.P. (1998). The Eph family receptors and ligands. Pharmacol. Ther. *77*, 151–181.